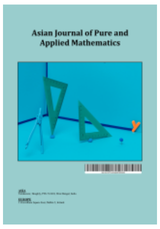

Asian Journal of Pure and Applied Mathematics

Volume 6, Issue 1, Page 88-103, 2024; Article no.AJPAM.1421

Analysis of Heat Transfer on Magnetohydrodynamic Hybrid Nanofluid Flow over a Permeable Stretching Surface in a Porous Medium

A. J. Tsokojo [a*], P. O. Olanrewaju [a] and D. O. Ogwumu [a]

[a] Department of Mathematics and Statistics, Federal University Wukari, Taraba State, Nigeria.

Authors' contributions

This work was carried out in collaboration among all authors. All authors read and approved the final manuscript.

Article Information

Open Peer Review History:
This journal follows the Advanced Open Peer Review policy. Identity of the Reviewers, Editor(s) and additional Reviewers, peer review comments, different versions of the manuscript, comments of the editors, etc are available here: https://prh.globalpresshub.com/review-history/1421

Original Research Article

Received: 05/09/2023
Accepted: 11/11/2023
Published: 02/02/2024

Abstract

Hybrid nanofluids enhance heat transfer and thermal conductivity in various applications, from electronics cooling to solar energy collection. They offer energy efficiency benefits and can reduce material usage. Their use spans multiple industries, including electronics, energy, and medical treatments.In this paper we study theoretically the analysis of heat transfer on MHD hybrid nanofluid flow over a permeable stretching surface in a porous medium with variable viscosity and other physiochemical properties for detailed interpretation and usefulness of the fluid flow parameters in modelling. Uniform magnetic field is applied together with heat source and sink. Three set of different hybrid nanofluids with water as a base fluid having suspension of copper-Aluminium Oxide $(Cu - Al_2O_3)$, Silver-Aluminium Oxide $(Ag - Al_2O_3)$ and copper-Silver $(Cu - Ag)$ nanoparticles are considered. The maragoni boundary conditions applied. The governing models of the flow is solved by Runge-Kutta fourth order method with shooting technique, using appropriate similarity transformations. Temperature and velocity field are explained by the figures for many flow pertinent parameters. Almost same behavior is observed for all the parameters presented in

**Corresponding author: E-mail: tsokojo1@gmail.com;*

this analysis for the three set of hybrid nanofluids. It was also observed that Radiation, Heat source/Sink and Local temperature difference has no significant impact on the velocity profile. Also increase in mass transfer wall decreases both the velocity and temperature profile. Hence all the embedded fluid flow parameter of the hybrid nanofluid has greater influence on the skin friction, nusselt number and the thermal boundary layer.

Keywords: Heat transfer; magnetohydrodynamics; hybrids nanofluid, stretching sheet; runge kutta fourth order; shooting technique.

1 Introduction

"Hybrid nanofluid is a very new type of nanofluids that contains two or more various nano particles. they are prepared by bringing two different kinds of nanoparticles in the same basefluid to have better thermo physical, optical, rheological, and morphological properties. Hybrid nanofluids are design to take the place of simple nanofluids due to quite a reasonable fact such as wide absorption range, lower extinction, high thermal conductivity, low pressure drop, and low frictional losses and pressure compared to the mono nanofluids, However There are numerous applications in which hybrid nanofluids can be used and some of the highlighted areas are solar energy, refrigeration and heating, ventilation and air conditioning application, heat exchanger, heat pipes, coolant in marching and manufacturing, electronic cooling, automotive industry, generator cooling, transformer cooling, biomedical, space, ships and defence and many others [1]. Because of its wide application, its deems to have attracted a large interest of researcher; Turcu et al, [2] is one of the first researchers who have begun "studies on hybrid Nanoparticles, Maxwell liquid flow characteristics and usages are improved by the convective and conducting strength of the nanoliquid". "In this century, nanotechnology is a strong propelling force in the industry and technological exploring area" Hong et al. [4]. According to Agostini et al. [3] "Different techniques are utilized for cooling of components that PCM heat sink and fins but these techniques are insufficient for meeting the demand of thermal management of these components" Qureshi et al. [1]. The output parameters like maximum power output were considered by using various nano fluids to minimize heat dissipation of heat sink.

"Science of hybrid nanofluids is intricately determined due to the responses to particle specification, temperature base fluid, and surfactant and then, PH value. The thermophysical properties or an element such as thermal conductivity happens to differ with temperature, nano particles sizes and concentration. There is a noticeable fluctuation of particles size, concentration and PH with the viscosity of the hybrid nanofluids. The improved performance is caused by the steps of hybrid nanofluids" Shah and Ali, [5]. "Hybrid nanofluids are the new high-level class of working fluids in heat transfer applications. However, many studies are needed to make them adaptable with domestic and commercial applications and today study results on hybrid nanofluids are not strong enough for presented goal. In fact there are lots of problems in hybrid nano fluid preparation like stable and large-scale synthesize, etc. that needed to resolve. Despite many unsolved questions and problems about nanofluid and hybrid nanofluids, there are few researchers that have taken this responsibility and devoted all of power and equipments to answer the open questions about nano fluid and hybrid nanofluids. Along with common used nano particles in mono nanofluids, CNTs, graphene, ceramic oxides, etc. can be used next to them as second nano particle to reach desired properties by hybrid nanofluids" (Wcislik, [6]).

"The nanotechnology applications at cellular and molecular level have brought great improvement in the field of health care and life sciences" Godin et al. [7]. "It became the most imperative study in recent years. Nanofluids and NPs are widely used in biomedical sector. NPs have adhesion to tumor cells compared to normal cells and combined effect of radiations as well as hyperthermia is due to heat produced after repair process as radiations induced DNA damage" Sridhara et al. [8]) (Wong and Leon, [9]) studied "NPs are fastened with the aid of releasing anticancer medicine at fixed rate. The flow of fluid inside the channels exists in many natural and man-made systems. Heat and mass transfer occurs in the channels' walls of human body such as the brain, lung, kidney and also in engineering instruments such as heat exchangers, atomic reactors, and so on. The development of microelectromechanical devices requires miniaturized heat exchangers. For example, cooling the mirrors used in high-power laser systems, require cooling systems that cover very small surfaces. Advances in genetic engineering and biomedical engineering require precise control of the transfer of heat and fluid in channels with micrometer dimensions". "An appropriate understanding of fluid flow and heat transfer in these microscale systems is needed to design and exploit them. The use of smaller-sized channels, although having a higher pressure drop, can increase heat transfer for temperature controlling goals such as transmitting and carrying live and coarse biological molecules that need for appropriate storage conditions" according to (Chein and Chuang, [10]).

"The problem of MHD stagnation point flow over a stretching sheet with fluid rotation and heat generation was considered, the dimensionless parameter enhance the velocity profile because of buoyancy effect and its dropped in the other profile because of drag force" (Wunuji et.al, [11]). "Heat conduction, is also referred to as diffusion, the direct microscopic exchange of kinetic energy of particles through the stationary boundary between two systems. Heat conduction occurs between stationary masses where there is no movement to carry heat away. Heat convection occurs when bulk flow of fluids (gas or fluids) carries heat along with the flow of matter in the fluid. The flow of fluid may be forced by external processes or sometimes (in gravitational fields) by buoyancy forces caused when thermal energy expands in fluid, thus influencing its own transfer. The later process is sometimes called"natural convection"by" (Kelvin, [12]). "The final major form of heat transfer is by radiation which occurs in any transparent medium but may also occur vacuum. Radiation is the transfer of energy through space by means of electromagnetic waves in much the same way as electromagnetic light waves transfer light. Heat transfer methods are used in numerous disciplines, such as automotive engineering, thermal management of electronic devices and system, climate control, insulation, material processing and power plant engineering. various mathematical methods have been developed to solve the results of heat transfer in system" [12].

(Abu-Nada and Oztop, [13]) "numerically investigated the effect of fluid flow and natural convective heat transfer inside a two-dimensional enclosure filled with water-based copper (Cu) nanofluid varying the inclination angle (1-20 degrees) and particle concentration. Finite volume method was used to solve the governing equations and found that the augmentation in Nusselt number (Nu) was more prominent at low particle volume fraction than that of high concentration. A substance or medium that have continuous pores through which fluid can flow is known as porous medium. Metal foams, ceramics, sand, and composite materials are few examples of porous medium, which have applications in cooling of electronic parts, high efficiency insulators and geothermal systems, etc. To improve heat transfer characteristics of porous media, researchers are employing hybrid nanofluid".

2 Problem Formulation

This study considered the two-dimensional viscous incompressible boundary layer Marangoni convective flows of three hybrid nanofluids over a permeable stretching surface with variable viscosity and constant thermal heat conductivity. Three set of different hybrid nanofluids with water as a base fluid having suspension of Copper-Aluminum Oxide (Cu - Al_2O_3), Silver-Aluminum Oxide (Ag - Al_2O_3) and Copper-Silver (Cu - Ag) nanoparticles will be considered. Similarly, the laminar flow and thermal equilibrium state of the fundamental fluids and the nano-size particles is also considered. The flow of nanofluids is presumed at $y \geq 0$ where x-axis is considered on the surface and y-axis is assumed normal to the surface as depicted in Fig. 1 below.

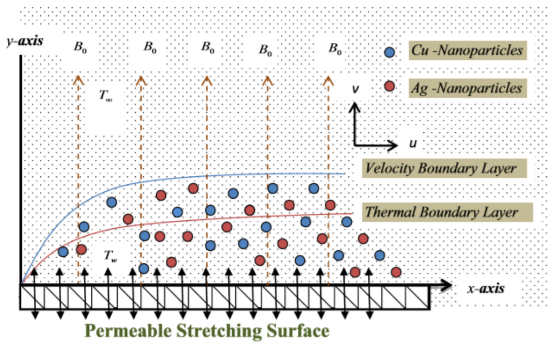

Picture 1. Permeable stretching surface (Agrawal et al, 2021)

"Here temperature T_∞, as free stream and T_w, at the surface are not same. Unidirectional magnetic field with heat sink/source applied perpendicular to surface. Porous medium with permeable surface is also considered. Furthermore, the surface tension varying, with T, linearly as we have assumed Marangoni convection" (Ganesh et al, [14] and Agrawal et al, [15]):

$$\gamma = \gamma_0\left[1-\bar{\gamma}\left(T-T_\infty\right)\right].$$

In the above equation, at interfaces, surface tension is γ_0 and $\bar{\gamma}$ is the changing rate of surface tension with T. considering above assumed conditions; the mathematical model of the flow is given by the following partial differential equations

$$\frac{\partial u}{\partial x}+\frac{\partial v}{\partial y}=0 \tag{1}$$

$$\frac{\partial u}{\partial t}+u\frac{\partial u}{\partial x}+v\frac{\partial u}{\partial y}=\frac{1}{\rho_{hnf}}\frac{\partial}{\partial y}\left(\mu_{hnf}\frac{\partial u}{\partial y}\right)-\frac{\sigma_{hnf}}{\rho_{hnf}}B_o{}^2u-\frac{\mu_{hnf}}{\rho_{hnf}}\frac{u}{k} \tag{2}$$

$$\begin{aligned}\frac{\partial T}{\partial t}+u\frac{\partial T}{\partial x}+v\frac{\partial T}{\partial y}=\frac{K_{hnf}}{\left(\rho C_p\right)_{hnf}}\left(\frac{\partial^2 T}{\partial y^2}\right)-\frac{1}{\left(\rho C_p\right)_{hnf}}\left(\frac{\partial q_r}{\partial y}\right)\\ +\frac{Q_o}{\left(\rho C_p\right)_{hnf}}\left(T-T_\infty\right)+\frac{\sigma_{hnf}}{\left(\rho C_p\right)_{hnf}}B_o{}^2u^2\end{aligned} \tag{3}$$

In the right hand side (RHS) of equation (2), first term represent solutal diffusion parameter, second term represents magnetic field parameter and third term stands for porous medium effect. The first, second, third and fourth terms on the RHS of equation (3) denote the thermal diffusion parameter, radiation, heat sink/source and magnetic effects, respectively.

The boundary conditions under the above assumptions are stated as follows

$$\begin{aligned}&v=v_w,\quad T=T_\infty+bx^2,\quad \mu_{hnf}\left(\frac{\partial u}{\partial y}\right)=\frac{\partial\sigma}{\partial T}\frac{\partial T}{\partial x}\ at\ y=0,\\ &u\to 0,\ T\to T_\infty\qquad as\ \ y\to\infty.\end{aligned} \tag{4}$$

Where velocity components along x and y axis, are taken as u and v, respectively, also μ_{hnf} is the viscosity of hybrid nanofluid, k_{hnf} is the thermal conductivity, ρ_{hnf} is the density, k is the coefficient of porosity, σ_{hnf} is the electrical conductivity and $\left(\rho C_p\right)_{hnf}$ is the heat capacity. "Here, subscript hnf, nf and f defined for hybrid-nanofluids, nanofluids and base fluid, respectively. Magnetic field is B_o and heat flux by radiation is represented by q_r. By the Roseland approximations, heat flux radiation q_r is considered" (Olanrewaju et al.., [16]):

$$q_r = -\frac{4\sigma *}{3k *}\frac{\partial T^4}{\partial y} = -\frac{16\sigma *}{3k *}T_\infty{}^3\frac{\partial T}{\partial y} \qquad \text{(a)}$$

Where $\sigma *$ represents the Stefan-Boltzman constant and mean absorption coefficient is $k*$

3 Similarity Transformation

For the solution of the model we applied similarity transformation as follows:

$$\eta = \left(\frac{a}{\nu}\right)^{1/2} y, \quad \theta(\eta) = \frac{T - T_\infty}{T_w - T_\infty}, \; \varphi = (a\nu)^{1/2} x f(\eta), \qquad (5)$$

when variable viscosity μ is a linear function of the form $\frac{\mu_\infty}{[1+\gamma(\mathrm{T}-\mathrm{T}_\infty)]}$

Introducing the transformation (5) into (1) to (4) we obtained the simplified form as

$$f''-\Omega_1\,\theta' f''+\mathrm{B}(1+\Omega\theta)\left[ff''-(f')^2\right]-\mathrm{M}(1+\Omega\theta)f'-\mathrm{AK}_1 f' \qquad (6)$$

$$\frac{1}{\Pr}\left[1+\frac{4R}{3}\right]\theta''+\delta\,\theta+f\theta'+\mathrm{M}\,\lambda_2\,(f')^2=0 \qquad (7)$$

$$f'''-\Omega_1\theta' f''+B(1+\Omega\theta)\left[f-\frac{c_1}{2}\eta\right]f''-B(1+\Omega\theta)(f')^2-M(1+\Omega\theta)f'-\mathrm{AK}_1 f'=0 \qquad (8)$$

$$\frac{1}{\rho r}\left[1+\frac{4R}{3}\right]\theta''+\delta\theta+\left[f-\frac{c_1}{2}\eta\right]\theta'+M\lambda_2(f')^2=0 \qquad (9)$$

with its corresponding boundary conditions

$$\theta(0)=1,\; f(0)f_w,\; f''(0)=-\frac{1}{2},\theta(\infty)=0,\; f'(\infty)=0 \qquad (10)$$

Where η, $f(\eta)$, $\theta(\eta)$ are the governing Non-dimensional distance,velocity and Temperature respectively

Here; $\Omega_2 = \frac{\Omega}{1+\Omega\theta_1}$, $B = \frac{\rho\nu}{\mu_0(1-ct)^2}$, $\Omega = \gamma\mathrm{T}_\infty$, $\mathrm{M} = \frac{\delta\beta_0^2}{\rho CP}$, $A = \frac{\nu}{a}$, $c_1 = \frac{c}{a}$, $K_1 = \frac{1}{ak}$

$R = \frac{4\sigma T_\infty^3}{\kappa_f}$ $\Pr = \frac{pc_p\nu_f}{k_f}$ $\sigma = \frac{Q_0}{apc_p}$ are the governing dimensionless parameter, modified viscosity variation,modified fluid density,viscosity variation,magnetic parameter, magnetic parameter, modified kinematic viscosity, similarity variables fluid constant, permeability, radiation parameter, Prandtl. Number, heat/source parameter respectively.

4 Results and Discussion

Equation (6) to (9) alongside with equation (10) have been solved using fourth order Runge kutta Method and shooting method however the tabular and graphical representation of this pertinent parameters like the Non-dimensional and dimensionless parameter would be depicted in Table 1and Figs 1 to 19 respectively.

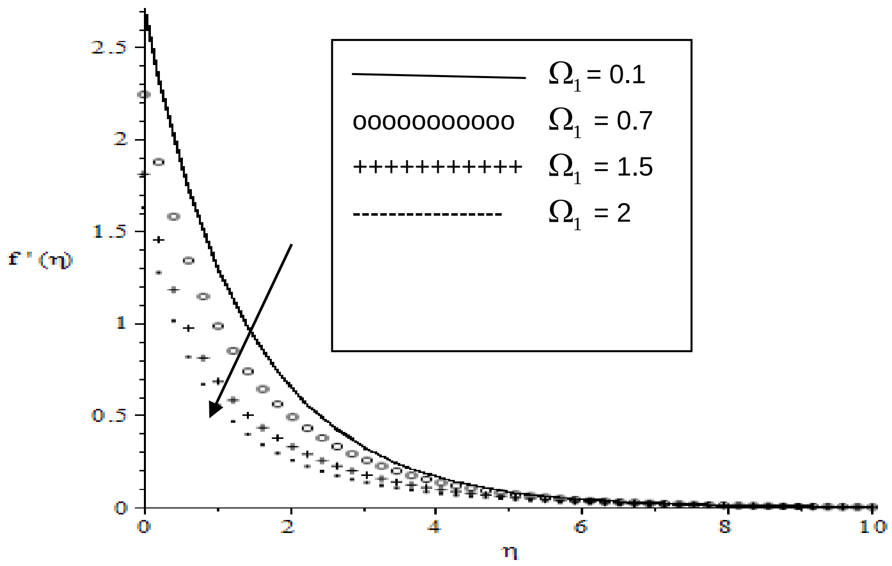

Fig. 1. Effect of modified viscosity variation parameter on velocity profile for fixed values of Ω = B = M = k_1 = R = $\sigma = \Omega_2$ = f_w = 0.1, A = 1, Pr = 0.72

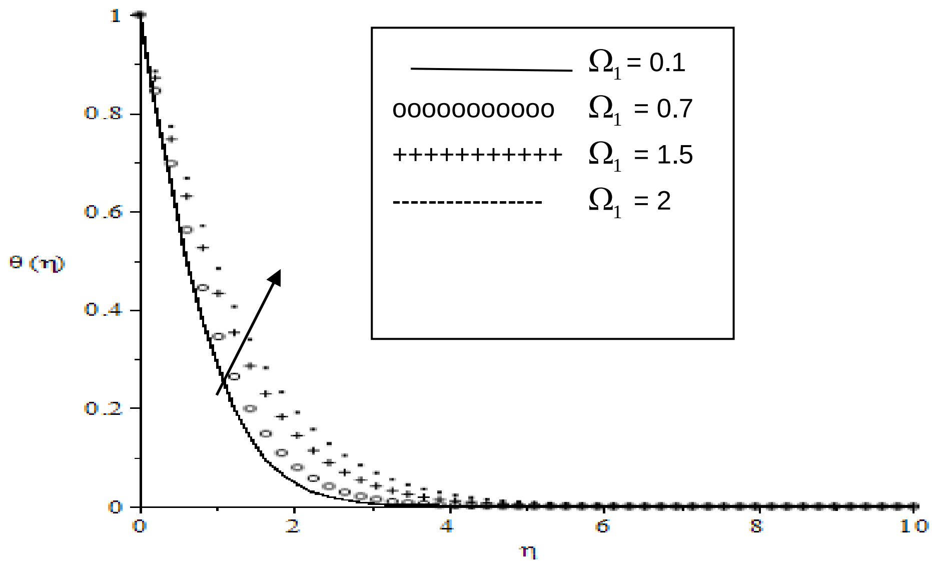

Fig. 2. Effect of modified viscosity variation parameter on temperature profile for fixed values of Ω = B = M = k_1 = R = $\sigma = \Omega_2$ = f_w = 0.1, A = 1, Pr = 0.72

Table 1. When variable viscosity is a linear function

λ_1	**B**	**M**	**A**	**K1**	**R**	**Pr**	σ	λ_2	***Fw***	λ	$-\theta'(0)$	$-f''(0)$
1	0.1	0.1	1	0.1	0.1	0.72	0.1	0.1	0.1	0.1	0.709803897022366	2.00000000000000
2	0.1	0.1	1	0.1	0.1	0.72	0.1	0.1	0.1	0.1	0.563038592529499	2.0000000000000
3	0.1	0.1	1	0.1	0.1	0.72	0.1	0.1	0.1	0.1	0.453973069780275	2.0000000000000
1	0.4	0.1	1	0.1	0.1	0.72	0.1	0.1	0.1	0.1	0.536622433033236	2
1	0.8	0.1	1	0.1	0.1	0.72	0.1	0.1	0.1	0.1	0.414560405599153	2
1	0.1	0.5	1	0.1	0.1	0.72	0.1	0.1	0.1	0.1	0.537277953163926	2.00000000000000
1	0.1	1	1	0.1	0.1	0.72	0.1	0.1	0.1	0.1	0.404013358999555	2
1	0.1	1.5	1	0.1	0.1	0.72	0.1	0.1	0.1	0.1	0.307368726586344	2.00000000000000
1	0.1	0.1	2	0.1	0.1	0.72	0.1	0.1	0.1	0.1	0.466564122721668	1
1	0.1	0.1	3	0.1	0.1	0.72	0.1	0.1	0.1	0.1	0.318787507430894	1.00000000000000
1	0.1	0.1	4	0.10.1	0.1	0.72	0.1	0.1	0.1	0.1	0.207393198748237	0.500000000000000
1	0.1	0.1	1	0.5	0.1	0.72	0.1	0.1	0.1	0.1	0.570541248392351	2.000000000000000
1	0.1	0.1	1	1	0.1	0.72	0.1	0.1	0.1	0.1	0.455029754438759	2.000000000000000
1	0.1	0.1	1	2	0.1	0.72	0.1	0.1	0.1	0.1	0.296914531802767	2
1	0.1	0.1	1	0.1	0.4	0.72	0.1	0.1	0.1	0.1	0.595280840563870	2.00000000000000
1	0.1	0.1	1	0.1	0.7	0.72	0.1	0.1	0.1	0.1	0.518217536660117	2.00000000000000
1	0.1	0.1	1	0.1	1	0.72	0.1	0.1	0.1	0.1	0.461793238215415	2.00000000000000
1	0.1	0.1	1	0.1	0.1	3	0.1	0.1	0.1	0.1	1.57392167565397	2.00000000000000
1	0.1	0.1	1	0.1	0.1	7.1	0.1	0.1	0.1	0.1	2.55625173738799	2
1	0.1	0.1	1	0.1	0.1	0.72	0.5	0.1	0.1	0.1	0.517580152427070	2.00000000000000
1	0.1	0.1	1	0.1	0.1	0.72	1	0.1	0.1	0.1	0.177736841437091	2.00000000000000
1	0.1	0.1	1	0.1	0.1	0.72	0.1	0.5	0.1	0.1	0.662137682996970	2.00000000000000
1	0.1	0.1	1	0.1	0.1	0.72	0.1	1	0.1	0.1	0.600815926460819	2.00000000000000
1	0.1	0.1	1	0.1	0.1	0.72	0.1	2	-0.1	0.1	0.384017000836725	2.00000000000000
1	0.1	0.1	1	0.1	0.1	0.72	0.1	0.1	-0.3	0.1	0.563849471982905	2.00000000000000
1	0.1	0.1	1	0.1	0.1	0.72	0.1	0.1	0.2	0.1	0.748831800247128	2.00000000000000
1	0.1	0.1	1	0.1	0.1	0.72	0.1	0.1	0.3	0.1	0.788829515865604	2.00000000000000
1	0.1	0.1	1	0.1	0.1	0.72	0.1	0.1	0.5	0.1	0.871631382083183	2.00000000000000
1	0.1	0.1	1	0.1	0.1	0.72	0.1	0.1	0.1	0.5	0.685067372165988	2.00000000000000
1	0.1	0.1	1	0.1	0.1	0.72	0.1	0.1	0.1	1	0.656270163236344	2.00000000000000
1	0.1	0.1	1	0.1	0.1	0.72	0.1	0.1	0.1	2	0.604312326328465	2.00000000000000

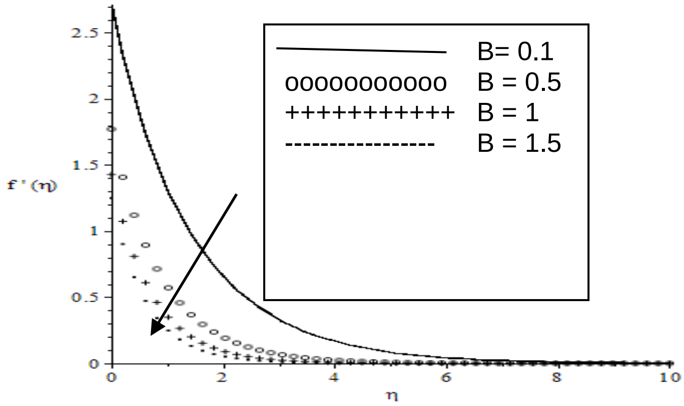

Fig. 3. Effect of modified fluid density parameter on velocity profile for fixed values of Ω_1 = M = k_1 Ω = R = $\sigma = \Omega_2$ = f_w = 0.1, A = 1, Pr = 0.72

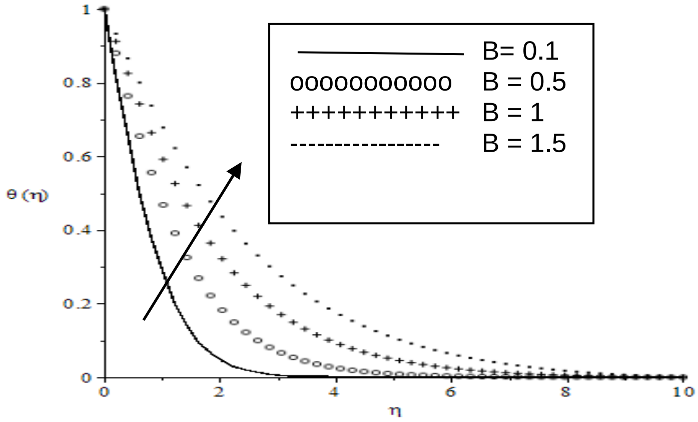

Fig. 4. Effect of modified fluid density parameter on temperature profile for fixed values of Ω_1 = M = k_1 Ω = R = $\sigma = \Omega_2$ = f_w = 0.1, A = 1, Pr = 0.72

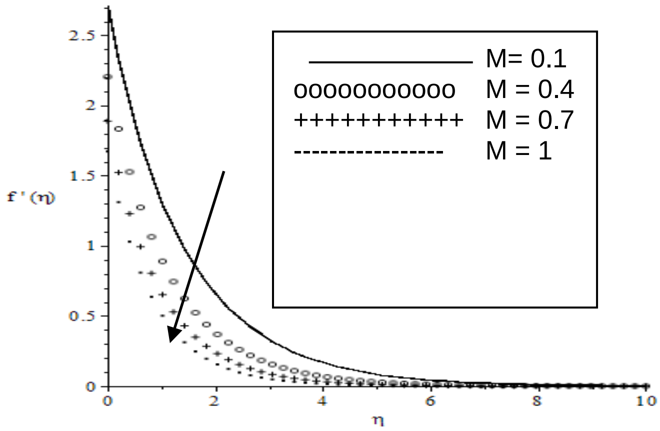

Fig. 5. Effect of magnetic field parameter on velocity profile for fixed values of Ω_1 = B = k_1 = Ω = R = $\sigma = \Omega_2$ = f_w = 0.1, A = 1, Pr = 0.72

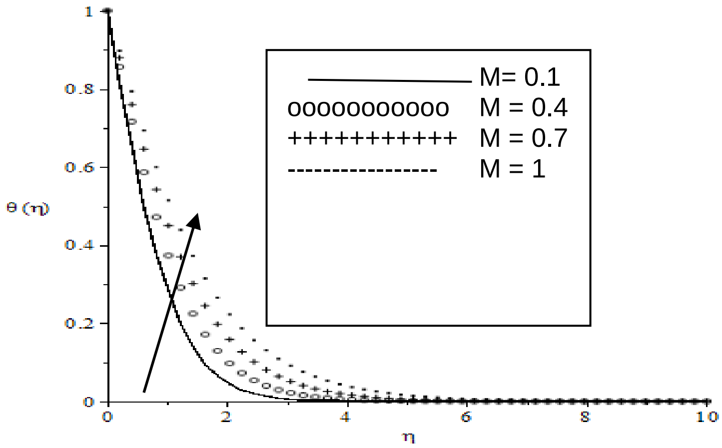

Fig. 6. Effect of magnetic field parameter on temperature profile for fixed values of Ω_1 = B = k1 = Ω = R = $\sigma = \Omega_2$ = f_w = 0.1, A = 1, Pr = 0.72

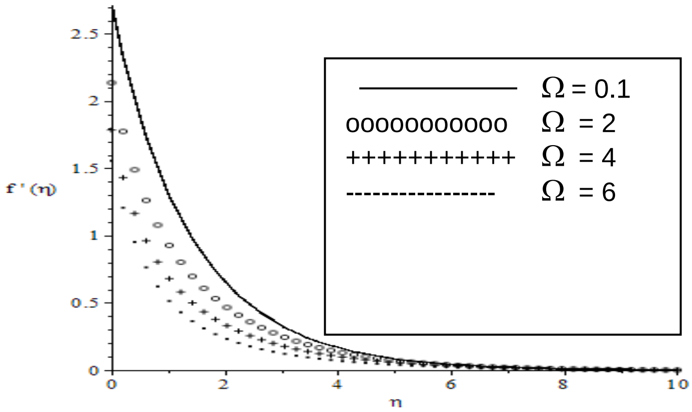

Fig. 7. Effect of viscosity variation parameter on velocity profile for fixed values of Ω_1 = B = k1 =M= R = $\sigma = \Omega_2$ = f_w = 0.1, A = 1, Pr = 0.72

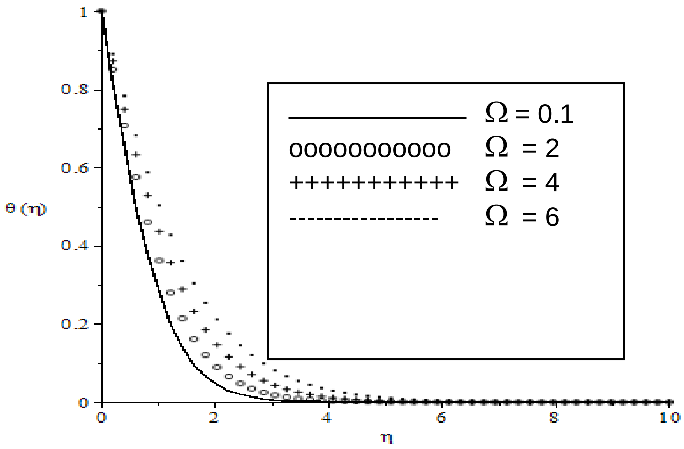

Fig. 8. Effect of viscosity variation parameter on temperature profile for fixed values of Ω_1 = B = k1 =M= R = $\sigma = \Omega_2$ = f_w = 0.1, A = 1, Pr = 0.72

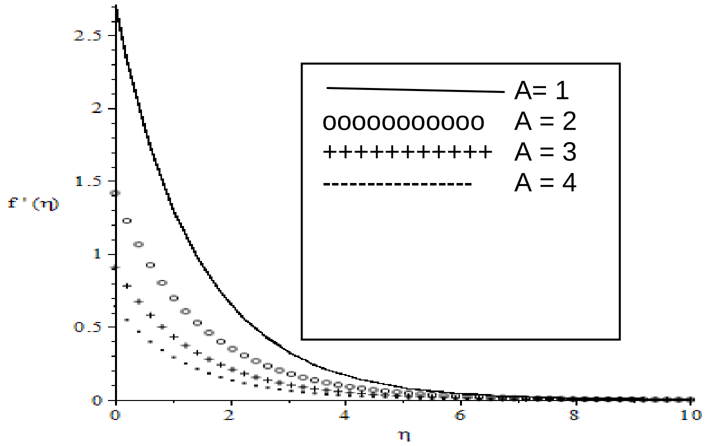

Fig. 9. Effect of modified kinematic viscosity parameter on velocity profile for fixed values of Ω_1 = B = k_1 =M= R = $\sigma = \Omega_2$ = f_w = 0.1, Ω =0.1, Pr = 0.72

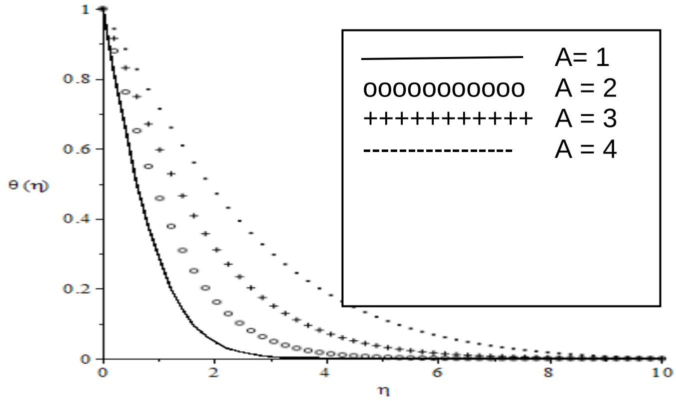

Fig. 10. Effect of modified kinematic viscosity parameter on temperature profile for fixed values of Ω_1 = B = k_1 =M= R = $\sigma = \Omega_2$ = f_w = 0.1, Ω =0.1, Pr = 0.72

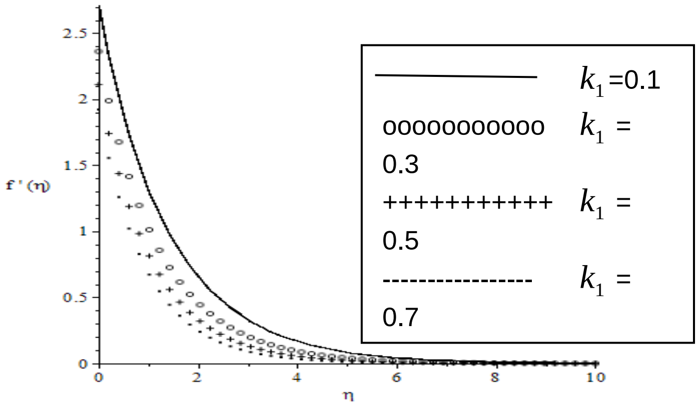

Fig. 11. Effect of permeability parameter on velocity profile for fixed values of Ω_1 = B =M= R = $\sigma = \Omega_2$ = f_w = 0.1, Ω =0.1, Pr = 0.72, A =1

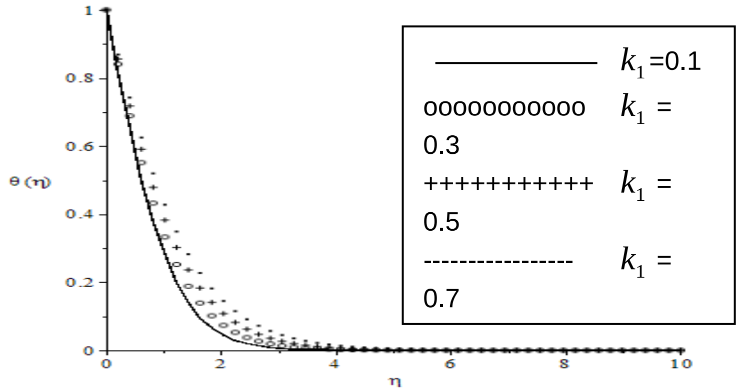

Fig. 12. Effect of permeability parameter on temperature profile for fixed values of Ω_1 = B =M= R = $\sigma = \Omega_2$ = f$_w$ = 0.1, Ω =0.1, Pr = 0.72, A =1

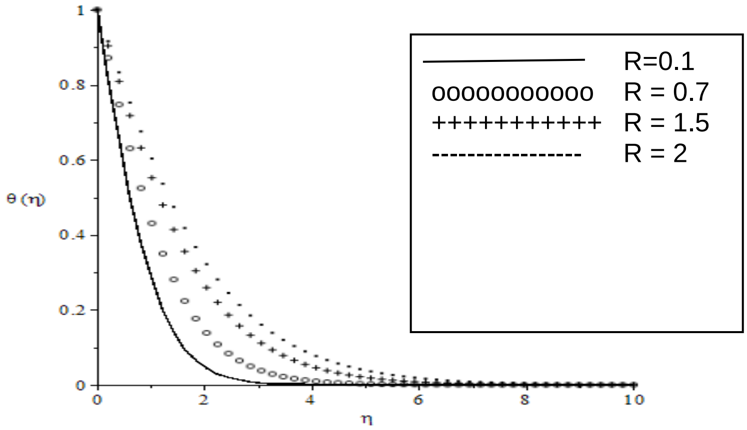

Fig. 13. Effect of radiation parameter on temperature profile for fixed values of Ω_1 = B =M= k_1 = $\sigma = \Omega_2$ = f$_w$ = 0.1, Ω =0.1, Pr = 0.72, A =1

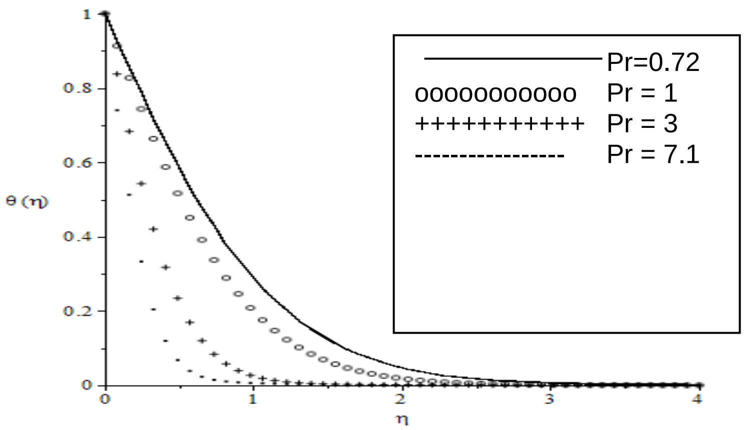

Fig. 14. Effect of Prandtl number on temperature profile for fixed values of Ω_1 = B =M= k_1 = R = $\sigma = \Omega_2$ = f$_w$ = 0.1, Ω =0.1, A =1

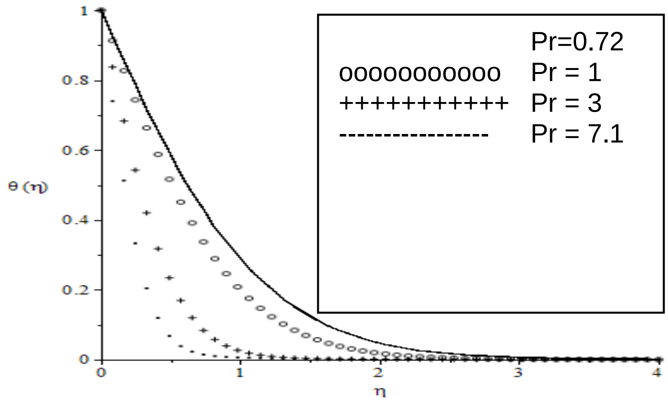

Fig. 15. Effect of Prandtl number on temperature profile for fixed values of Ω_1 = B =M= k_1 = R = $\sigma = \Omega_2$ = f_w = 0.1, Ω =0.1, A =1

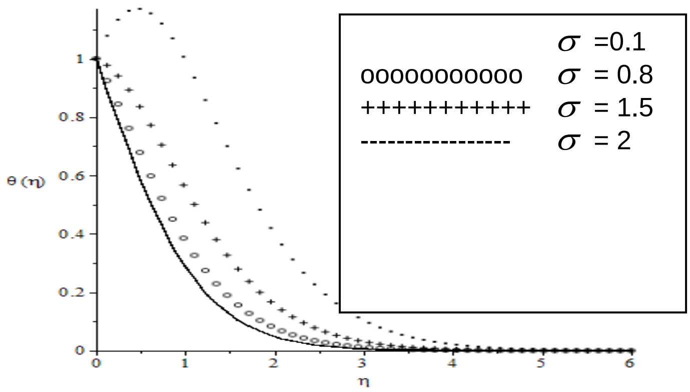

Fig. 16. Effect of heat sink/source on temperature profile for fixed values of Ω_1 = B =M= k_1 = R = Ω_2 = f_w = 0.1, Ω =0.1, A =1, Pr = 0.72

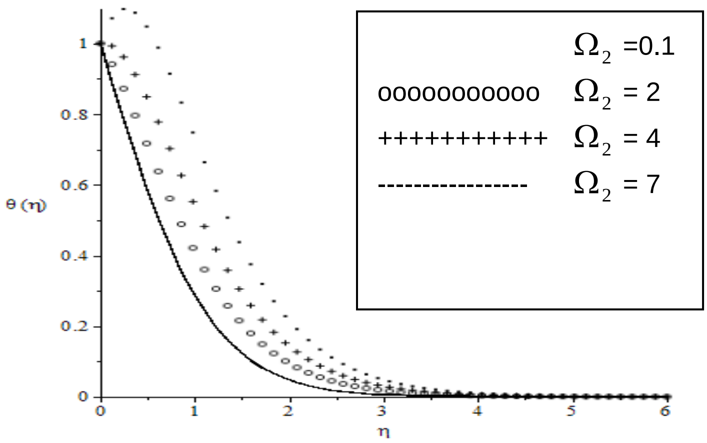

Figure 17: Effect of local temperature difference on temperature profile for fixed values of Ω_1 = B =M= k_1 = R = σ = f_w = 0.1, Ω =0.1, A =1, Pr = 0.72

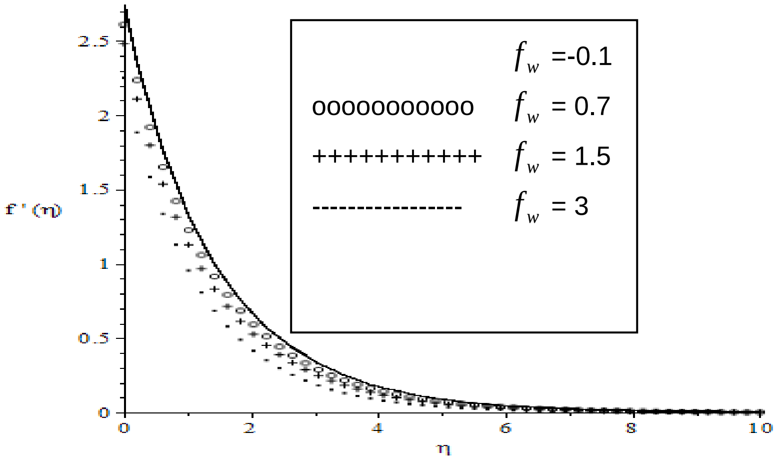

Fig. 18. Effect of mass transfer wall parameter on velocity profile for fixed values of Ω_1 = B =M= k_1 = R = σ = Ω_2 = 0.1, Ω =0.1, A =1, Pr = 0.72

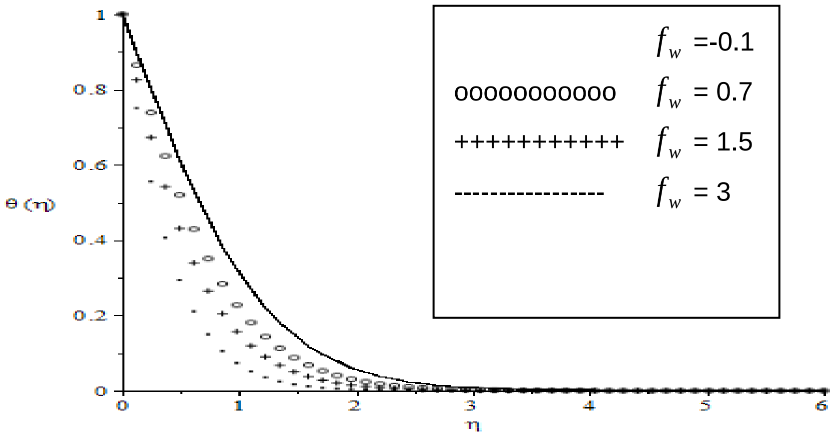

Fig. 19. Effect of mass transfer wall parameter on temperature profile for fixed values of Ω_1 = B =M= k_1 = R = σ = Ω_2 = 0.1, Ω =0.1, A =1, Pr = 0.72

Table 1 When variable viscosity is a linear function:

It has been clearly observed that as we vary the values of $\lambda_1, B, M, A, k_1, R, \delta, \lambda_2,$ The nusselt number decreases the thickness in the thermal boundary layer while the values of Pr and f_w increases towards the flow boundary layer. Similarly, as we increase λ_1, B, M, A, k_1, R, δ, λ_2, λ the skin friction remains constant because of the condition. Again, as we increase A the skin friction decreases towards the wall plate.

When variable viscosity is a linear function:

Fig. 2 Represents the effect of modified viscosity variation parameter on velocity profile for other parameters kept constant. It is observed from the graph that increase in the modified viscosity variation parameter decreases the fluid and dust phase velocities. Fig. 3 Shows that increase in modified viscosity variation parameters increases the temperature profile of both phases Fig. 4 is the effect of modified fluid density on velocity profile. Increasing modified fluid density leads to decrease in the flow velocity while, in Fig. 5; it indicate that increasing modified fluid density led to increase in the temperature profile. Fig. 6 It is observed that velocity of the flow decreases significantly throughout the fluid domain with increasing values of magnetic field parameters. Application of a magnetic field to an electronically conducting fluid produces a kind of drag-like force called Lorentz force. In Fig. 7: it shows that increase in the magnetic field parameters increase in the temperature profile in the entire domain. Fig. 8 Increase in the viscosity variation parameter decreases the fluid and dust phase velocities. Fig. 9 whereas increase in viscosity variation parameter increases the temperature profile of both the phases. Fig. 10 depict the effect of modified kinematic viscosity parameter on velocity profile. It shows clearly that the velocity profile is declining as the modified kinematic viscosity parameter increases. Meanwhile, Fig. 11: Increase in modified kinematic viscosity leads to increase in the temperature profile. Fig. 12 depicted the effect of increasing permeability parameter that led to decreasing the velocity profile of the porous materials. Also, Fig. 13 shows the effect of increasing permeability parameter contributes to the thickness of thermal boundary layer.

Fig. 14 It is noticed that with an augmentation in radiation we see an increment in temperature profile. Thermal radiation produces extra heating that led to increase temperature field. Moreover, radiation has not significant impact on the velocity profile. As can be seen in Fig. 15, as the prandtl number increases, temperatures decrease. The thickness of the thermal boundary layer decreases as the prandtl number rises. The connection between momentum and thermal diffusivity can be calculated using the prandtl number. The distribution of velocities shows almost no change as a function of the Prandtl number. Fig. 16 shows that as the hat source/sink parameter is increased, the resulting temperature profile is also increased. In addition, the mass fraction field is enhanced by a positive fluctuation in a species diffusivity parameter. The velocity distribution is unaffected by the presence or absence of a heat sink or source. As seen in Fig. 17, the temperature profile grew as the local temperature differential grew. There is little to no effect on the speed distribution from the local temperature gradient. The influence of the mass transfer wall parameter on the velocity and temperature profile is shown in Figs. 18 and 19. It is observed that the velocity profile and the thermal boundary layer both decrease with increasing mass transfer wall.

5 Conclusion

In this paper, we considered analysis of heat transfer on MHD hybrid Nano fluids flow over a permeable stretching surface in a porous medium. Uniform magnetic field is applied with heat sink/source. Three hybrid Nano fluids with water as a base fluid having suspension of copper-Aluminum oxide ($Cu - Al_2O_3$), silver-Aluminum oxide ($Ag - Al_2O_3$) and copper-silver ($Cu - Ag$) nanoparticles are considered. The set of governing equations and the boundary condition are reduced to ordinary differential equations with appropriate boundary conditions. The influence of all the parameters used are discussed in details. It has been observed from our computation that as we increase the value of $\lambda_1, B, M, A, k_1, R, \delta, \lambda_2$ the nusselt number decreases the thickness in the thermal boundary layer while increase in the value of Pr and f_w the nusselt number increases.

Competing Interests

Authors have declared that no competing interests exist.

References

[1] Qureshi ZA, Ali HM, Khushnood S. Recent advances on thermal conductivity enhancement of phase change materials for energy storage system: a review. International Journal of Heat and Mass Transfer. 2018;127:838-856.

[2] Turcu R, Darabont AL, Nan A, Aldea N, Macovei D, Bica D, et al. New polypyrrole-multiwall carbon nanotubes hybrid materials. Journal of Optoelectronics and Advanced Materials. 2006;8(2):643-647.

[3] Hong TK, Yang HS, Choi CJ. Study of the enhanced thermal conductivity of Fe nanofluids. Journal of Applied Physics. 2005;97(6).

[4] Agostini B, Fabbri M, Park JE, Wojtan L, Thome JR, Michel B. State of the art of high heat flux cooling technologies. Heat Transfer Engineering. 2007;28(4):258-281.

[5] Shah TR, Ali HM. Applications of hybrid nanofluids in solar energy, practical limitations and challenges: A critical review. Solar Energy. 2019;183:173-203.

[6] Wciślik S. Efficient stabilization of mono and hybrid nanofluids. Energies. 2020;13(15):3793.
Poland; XXXX@tu.kielce.pl.

[7] Godin B, Sakamoto JH, Serda RE, Grattoni A, Bouamrani A, Ferrari M. Emerging applications of nanomedicine for the diagnosis and treatment of cardiovascular diseases. Trends in Pharmacological Sciences. 2010;31(5):199-205.

[8] Sridhara V, Gowrishankar BS, Snehalatha, Satapathy LN. Nanofluids—a new promising fluid for cooling. Transactions of the Indian Ceramic Society. 2009;68(1):1-17.

[9] Wong KV, De Leon O. Applications of nanofluids: current and future. Advances in Mechanical Engineering. 2010;2:519659.

[10] Chein R, Chuang J. Experimental microchannel heat sink performance studies using nanofluids. International Journal of Thermal Sciences. 2007;46(1):57-66.

[11] Wunuji AS, Yusuf A, Micheal BS, Aiyesimi YM. Magnetohydrodynamics (MHD) Stagnation Point Flow on a Stretching Sheet with Fluid Rotation and Heat Generation. Asian Journal of Pure and Applied Mathematics. 2023;274-284.

[12] Kelvin H. Heat Transfer Introduction. School of Chemical and metallurgical Engineering, University of the Witwatersrand, Johernesburg (south- Africa); 2018.

[13] Abu-Nada E, Oztop HF. Effects of inclination angle on natural convection in enclosures filled with Cu–water nanofluid. International Journal of Heat and Fluid Flow. 2009;30(4):669-678.

[14] Ganesh NV, Kameswaran PK, Al-Mdallal QM, Hakeem AK, Ganga B. Non-Linear thermal radiative marangoni boundary layer flow of gamma Al2O3 nanofluids past a stretching sheet. Journal of Nanofluids. 2018;7(5):944-950.

[15] Agrawal P, Dadheech PK, Jat RN, Baleanu D, Purohit SD. Radiative MHD hybrid-nanofluids flow over a permeable stretching surface with heat source/sink embedded in porous medium. International Journal of Numerical Methods for Heat & Fluid Flow. 2021;31(8):2818-2840.

[16] Olanrewaju AM, Salawu SO, Olanrewaju PO, Amoo SA. Unsteady radiative magnetohydromagnetic flow and entropy generation of maxwell nanofluid in a porous medium with arrhenius chemical kinetic. Cogent Engineering. 2021;8(1):1942639.

Peer-review history:
The peer review history for this paper can be accessed here (Please copy paste the total link in your browser address bar)
https://prh.globalpresshub.com/review-history/1421